guide increases, the light in the central guide gradually couples into the left (right) guide and the light from the right (left) guide is nearly unchanged. As can be seen from the Figure, when the reverse bias to the left (right) guide reaches -8 V, the largest guide coupling is achieved and the maximum optical switching from the central guide to left (right) output guide is observed. The total internal loss is 10·8 dB for a device with an 800 μm coupling length at the maximum optical switching. As the reverse bias to the left (right) guide increases further, the guide coupling is weakened and the output light intensity gradually decreases.

The near-field output intensity pattern for peak-to-peak switching is shown in Fig. 3. When the central and the left

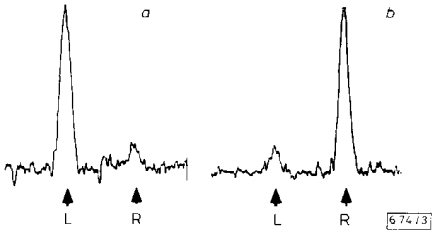

Fig. 3 *Near-field output intensity pattern of peak-to-peak switching characteristic for device with 4 μm-wide guides, 2 μm gaps between guides, and 800 μm coupling length*

a Output light from left output guide when central and left guides are created as -8 V is applied
b Output light from right output guide when central and right guides are created as -8 V is applied

guides are created, the input light couples into the left guide as mentioned before. Alternatively, when the right and central guides are created, the input light couples into the right guide. It is clear from Fig. 3 that a crosstalk of -10 dB is observed between the two output guides. In principle, the crosstalk should be zero because, while one side guide is turned on as the output, the other guide is extinguished. Another feature of the device is that the output light from the left and right guides is quite symmetric, which is very important in useful optical switches.

This optical switch with FIGs has an extra degree of freedom over conventional coupler switches because the coupling coefficient can be adjusted electrically. An arbitrary coupling length can always be adjusted for 100% coupling (if it meets a minimum coupling length requirement) by properly adjusting the DC guide voltage and modulating only one electrode. If the voltage applied to one side of the directional coupler is changed so that the coupling is spoiled, zero coupling will occur. We can scale the reference propagation constant of the system after fabrication so that errors in design length can be compensated for. This switch can operate over a large range of different wavelengths: the coupling length for different wavelengths can be matched due to the adjustable propagation constant of the waveguide. Because the switch is operated under reverse bias, the speed limitation imposed by carrier recombination times can be avoided.

In summary, we have fabricated and characterised a directional coupler optical switch. The device is constructed from three parallel field-induced waveguides. The experimental results show that by varying the applied biases to the output waveguides from 0 to -8 V, a switching characteristic between the two output ends with a crosstalk of -10 dB is achieved with 800 μm coupling length, operating at 1·15 μm wavelength.

13th October 1992

T. C. Huang and G. J. Simonis (*Army Research Laboratory, Adelphi, MD 20783-1197, USA*)

L. A. Coldren (*Department of Electrical and Computer Engineering, University of California, Santa Barbara, CA 93106, USA*)

References

1 TAKEUCHI, H., NAGATA, K., KAWAGUCHI, H., and OE, K.: 'GaAs/AlGaAs directional coupler switch with submillimeter device length', *Electron. Lett.*, 1986, **23**, pp. 1241–1243

2 ZUCKER, J. E., JONES, K. L., YOUNG, M. G., MILLER, B. I., and KOREN, U.: 'Compact directional coupler switches using quantum well electrorefraction', *Appl. Phys. Lett.*, 1989, **55**, pp. 2280–2282

3 KOMATSU, K., HAMAMOTO, K., SUGIMOTO, M., AJISAWA, A., KOHGA, Y., and SUZUKI, A.: '4 × 4 GaAs/AlGaAs optical matrix switches with uniform device characteristics using alternating $\Delta\beta$ electrooptic guided-wave directional couplers', *J. Lightwave Technol.*, 1991, **LT-9**, pp. 871–878

4 HUANG, T. C., CHUNG, Y., DAGLI, N., and COLDREN, L. A.: 'GaAs/AlGaAs multiple quantum well field-induced optical waveguide', *Appl. Phys. Lett.*, 1990, **57**, pp. 114–116

NOVEL PACKET ARCHITECTURE FOR ALL-OPTICAL ULTRAFAST PACKET-SWITCHING NETWORKS

F. Forghieri, A. Bononi and P. R. Prucnal

Indexing terms: Optical communications, Packet switching

Header recognition and packet detection in all-optical networks using on/off optical ultrafast signalling at a fixed wavelength can be implemented by means of recently demonstrated optical sampling AND gates. A novel packet structure in which the header is spread in a TDM fashion over the optical packet allows the number of such AND gates to be minimised in the routing and receiving blocks thereby best exploiting the required electronics.

All-optical packet-switching networks take full advantage of the large bandwidth of the optical fibre because the transmitted signal remains in optical form from source to destination and electronic conversions occur only at the end points of the connection, so that ultrahigh bit rates may be used.

The bit rate matching between the ultrafast optical channel and the electronic receiver can be provided by using recently demonstrated optical sampling techniques and by paralleling the receiving electronics. Three different sampling techniques, all exploiting optical nonlinearities in the fibre, have recently been proposed to demodulate such ultrahigh bit rate data streams. They are based on the nonlinear optical loop mirror [1, 2], on soliton-trapping gates [3, 4], and on four-wave mixing [5]. A high power sampling optical pulse is synchronised on the desired bit slot in the incoming packet, to test whether a pulse is present or not. The sampler works as an optical AND gate, which yields the bit pulse when this is present, and no signal otherwise. The pulse at the output of the AND gate is then sent to a photodiode to be electronically detected.

These techniques may be used to read the header and demodulate the packet. With a parallel bank of optical samplers, packet detection is converted into the parallel detection of delta-like spikes at a repetition rate suitable for electronic detection.

A novel packet structure is proposed here to minimise the number of optical sampling gates in the header-recognition and packet-demultiplexing blocks. As shown in Fig. 1, the header, instead of preceding the payload, is spread regularly across the packet in a TDM fashion. If the interleaving period between header bits is longer than the minimum electronic detection time, the header can be extracted by sending the packet into a single AND gate together with an optical sampling clock at the interleaving rate. For example, ATM standards require a 53 byte packet, 48 bytes of which are for the payload, and 5 for the header. By inserting one header bit every 10 payload bits, a 55 byte packet is obtained where the two extra bytes added to the payload may be used for synchronisation purposes. If the desired optical bit rate in the packet is for instance 100 Gbit/s, the repetition rate of the

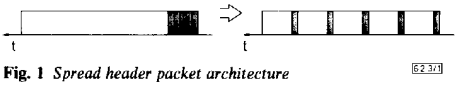

Fig. 1 *Spread header packet architecture*

spread header is below 10 Gbit/s, low enough to be handled by conventional optical receivers.

The implementation of packet generation, routing and detection tailored to the novel packet architecture will now be discussed.

Fig. 2 shows the optical packet generation block at the transmitting node. The electronic input is a packet with h

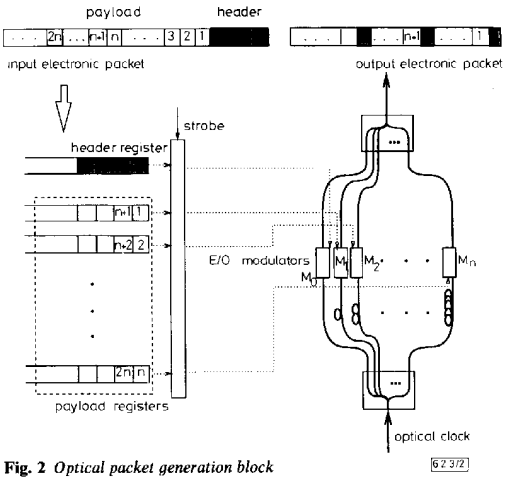

Fig. 2 *Optical packet generation block*

header bits and p payload bits, with p an integer multiple of h, $p = nh$. The header is extracted and serially fed into a dedicated shift register. The payload, instead, is sequentially separated into n parallel shift registers, as shown in the Figure. This initial process can be carried out at low electronic speed. A local optical clock generated by a mode-locked laser produces ultrashort optical pulses at a repetition rate

$$R_c = \frac{R}{n+1}$$

where R is the bit rate in the optical packet. The clock output is split into $n + 1$ fibre branches to obtain 1 bit shifted replicas of it, which are fed to an array of $n + 1$ electro-optic (E/O) modulators. Once the electronic packet separation is complete, a strobe signal starts the optical packet modulation. The $n + 1$ shift registers feed the parallel bank of modulators at a modulation rate equal to the clock rate R_c. The modulated optical pulses are recombined into a single stream to yield the optical packet in h clock periods.

Fig. 3 details the header recognition at the node. A fibre delay is inserted after the input coupler so that incoming packets are sensed before they arrive at the routing switch, long enough in advance to allow for the header to be read, the routing decisions to be made and the switch to be set. A small portion of the incoming optical packet is stripped off by the optical coupler and sent to the header recognition and routing block. A properly synchronised version of the same optical clock used for packet generation is optically 'ANDed' with this replica of the packet to extract the header bits, which are then detected by a fast photodiode (PD) and stacked into a fast-access shift register [6]. Processing of the register contents can be pipelined to perform the routing operations at a suitable electronic speed [7]. In this way the processing capability of the electronics is fully exploited.

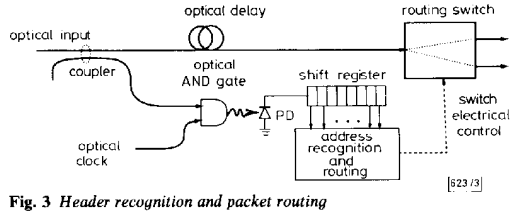

Fig. 3 *Header recognition and packet routing*

Fig. 4 shows the demultiplexer–receiver scheme. The same technique used to extract the header can be used to demultiplex and detect the payload. 1 bit shifted versions of the local

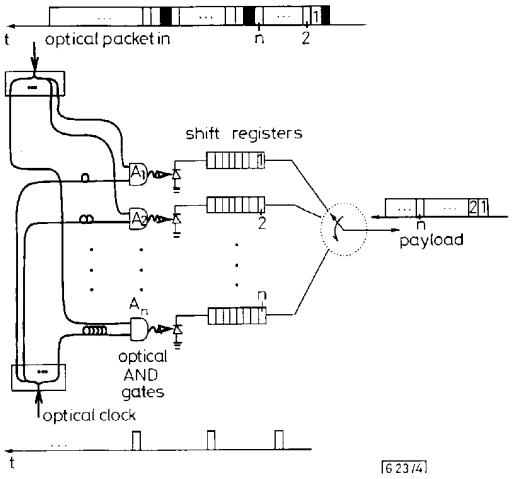

Fig. 4 *Scheme of demultiplexer–receiver*

sampling clock are sent to an array of n optical sampling gates together with the received packet to extract n interleaved pulse trains so that demultiplexing by a factor of n is achieved. Each of the n optically sampled sequences at rate R_c is sent onto a fast photodiode and electronically buffered. The output of the n electronic shift registers is finally sequentially scanned to obtain parallel-to-serial conversion and yield the received payload at lower electronic rates. The shift registers should have enough buffers to accommodate a stream of received back-to-back optical packets and thus match the ultrahigh rates of the network to the lower electronic output rates.

The optical sampling gates are the connecting link between the ultrafast optics and parallel electronics. With the proposed 'minimal' solution, electronic regeneration at intermediate nodes seems to be possible even at ultrahigh bit rates, thereby overcoming the classic electronic bottleneck. This can be obtained at no cost at active nodes, that is nodes capable of transmitting and receiving optical packets, which are already equipped with the necessary ultrafast interface, whereas passive switching nodes will have only one sampling gate if intermediate regeneration is not required.

Packet regeneration destroys the transparency property of nonregenerative all-optical networks, but allows the physical size of the network to be increased by avoiding accumulation of noise and distortion along the path of each optical packet.

The proposed schemes emphasise the use of electronic processing where an all-optical counterpart is not available at present. Only one optical AND gate is used in the header recognition block, and the number of demultiplexing branches n can be minimised for a given optical bit rate R by using the highest value of R_c allowed by the processing time of the slowest electronic block in the address recognition and routing pipe [7].

8th October 1992

F. Forghieri, A. Bononi and P. R. Prucnal (*Department of Electrical Engineering, Princeton University, Princeton, NJ 08544, USA*)

References

1 DORAN, N. J., and WOOD, D.: 'Nonlinear-optical loop mirror', *Opt. Lett.*, 1988, **13**, pp. 56–58

2 ANDREKSON, P. A., OLSSON, N. A., SIMPSON, J. R., DIGIOVANNI, D. J., MORTON, P. A., TANBUN-EK, T., LOGAN, R. A., and WECHT, K. W.: '64 Gb/s all-optical demultiplexing with the nonlinear optical-loop mirror', *IEEE Photonics Technol. Lett.*, 1992, **4**, pp. 644–647

3 ISLAM, M. N.: 'Ultrafast all-optical logic gates based on soliton trapping in fibers', *Opt. Lett.*, 1989, **14**, pp. 1257–1259

4 CHBAT, M. W., HONG, B., ISLAM, M. N., SOCCOLICH, C. E., and PRUCNAL, P. R.: 'Ultrafast soliton-trapping AND gate', to be published in *J. Lightwave Technol.*, December 1992
5 ANDREKSON, P. A., OLSSON, N. A., HANER, M., SIMPSON, J. R., TANBUN-EK, T., LOGAN, R. A., COBLENTZ, D., PRESBY, H. M., and WECHT, K. W.: '32 Gb/s optical soliton data transmission over 90 km', *IEEE Photonics Technol. Lett.*, 1992, **4**, pp. 76–79
6 HAUENSCHILD, J., REIN, H.-M., MCFARLAND, W., and PETTENGILL, D.: 'A silicon bipolar decision circuit operating up to 15 Gbit/s', *IEEE J. Solid-State Circuits*, 1991, **26**, pp. 1734–1736
7 PRUCNAL, P. R., and PERRIER, P. A.: 'Optically-processed routing for fast packet switching', *IEEE LCS*, 1990, **1**, pp. 54–67

INTEGRATED OPTIC LITHIUM NIOBATE IMAGE REJECTION CIRCUIT GIVING MINIMUM CHANNEL SPACING FOR 622 Mbit/s CPFSK LINK

R. Cush, N. Wood, P. T. Johnson, P. J. Duthie, C. Park and B. T. Debney

Indexing terms: Integrated optics, Optoelectronics, filters, Optical filters

A minimum channel spacing of 1·2 GHz has been achieved in a 622 Mbit/s CPFSK optical heterodyne link using image rejection. The image rejection circuit, which included a lithium niobate integrated 90° optical hybrid, provided over 23 dB of rejection and resulted in a greater than threefold increase in achievable channel density.

Introduction: Dense packing of optical channels, allowing full exploitation of the fibre bandwidth, can be achieved using coherent optical heterodyne detection. In practice, usable bandwidth is limited by the available tuning range of the local oscillator (LO) laser and so for applications requiring large channel numbers it is essential that the maximum packing density is obtained. However, heterodyne detection at the IF frequency prevents discrimination between the desired signal at $f_{LO}+f_{IF}$ (real) and the unwanted signal at $f_{LO}-f_{IF}$ (image). This results in the requirement for a much larger channel separation than that expected from the receiver filter passband width. The technique of image rejection allows the minimum channel spacing to be realised, by separating the real and image signals. This technique, common at microwave frequencies, has been demonstrated in the optical domain [1–3] using a variety of bulk optic and fibre optic arrangements. We present results for an integrated optic image rejection chip used within a coherent optical heterodyne data link. A reduction in channel spacing to the theoretical minimum [4] was achieved, corresponding to less than one third of that obtained without image rejection. We also consider the system tolerance to device fabrication variation.

Image rejection chip: The 90° optical hybrid function was achieved by controlling the polarisation of the transmitter and local oscillator so that the resulting TE and TM components of the mixed signal differ in phase by 90° (at the IF frequency) [1]. The sign of this phase difference depends on the optical frequency of the transmitter signal, i.e. whether it is on the real or image side. The TE and TM components are then separated and detected by separate receivers (Fig. 1) and the resulting IF signals are mixed using a 90° electrical hybrid. The additional 90° shift on one of the signals introduced by the electrical hybrid results in either addition or cancellation of the two components at the mixer output. As there is a total phase difference of 180° between the real and image signals on one of the components, if the real signals add, then the image signals must cancel. In this way the circuit may be set up to pass the real signal and reject the image signal. (In reality, the image signal appears on the second output port of the electrical hybrid).

In the testbed system, the 90° optical hybrid was provided by mixers and splitters integrated on a single lithium niobate chip. The chip was fabricated on X-cut lithium niobate, using

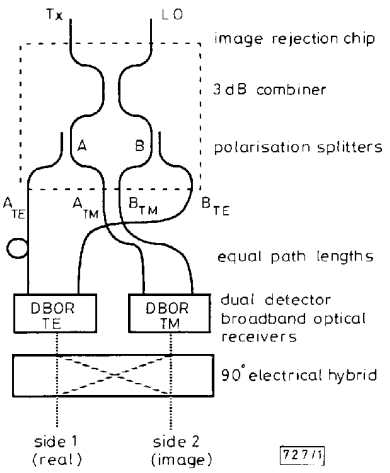

Fig. 1 *Configuration of image rejection circuit, with optical 90° hybrid*

standard titanium indiffusion processing techniques. The layout was designed to give equal path lengths on all routes through the chip, to ensure that the relative phase between components is preserved. The configuration is as shown in Fig. 1, and consists of a 3 dB splitter, followed by polarisation splitters. Four outputs are provided, two TE and two TM, for coupling to dual *pin* receivers. The rearrangement of the output port positions was achieved in the fibre link between the chip and the receivers. The chip was fibred using standard singlemode fibre to allow full control over the input polarisations. The insertion loss of the chip was measured to be $13{\cdot}4 \pm 1{\cdot}3$ dB for the LO arm and $12{\cdot}3 \pm 2{\cdot}3$ dB for the signal arm and the polarisation rejection was ≥ 10 dB.

Testbed system: A 622 Mbit/s CPFSK (modulation index, $m = 1$) data link was set up to enable the assessment of image rejection using two modulated transmitters. DFB MQW lasers were used for both the LO and transmitters. The two transmitters were combined using a fused fibre 3 dB coupler. A polarisation controller was incorporated in one transmitter arm, to facilitate the matching of the polarisation of the two transmitters. The combined transmitter signal was passed through a second polarisation controller, to allow manipulation of the combined polarisation, before being coupled into the image rejection chip. The output from the LO laser was passed through a third polarisation controller and an in-line half-wave plate before coupling into the image rejection chip.

The four outputs from the image rejection chip were coupled to two dual *pin* receivers, one receiver for the TE components and one for TM. The length of these connections was kept the same, to ensure preservation of the relative phase differences. The outputs from the two receivers, now at the IF frequency, were combined using a 90° hybrid. The resulting output is amplified and filtered before splitting, one output passing through a frequency discriminator for AFC, the other through a delay line data demodulator, then to the BER analyser. The two transmitter lasers were modulated at 622 Mbit/s using a 1010 data pattern.

Demonstration of image rejection: The simplest method of achieving the necessary phase differences required for image rejection is to combine a circularly polarised signal with one linearly polarised at 45° to the polarisation axes of the chip, although the same result may be achieved with other polarisation combinations. To achieve image rejection in the testbed system, the LO laser polarisation was adjusted so that it was linearly polarised along one polarisation axis. The orientation of the linear polarisation was then rotated using the half-wave plate to give 45° polarisation angle. The polarisation of the